

The Cracking Sensitivity of a Na-Geopolymer



Heng Sounean, Hannawi Kinda, and Darquennes Aveline

Abstract This research study aims to better understand the mechanical behavior of a Na-geopolymer used to immobilize the nuclear waste (MgZr alloys). Based on a large experimental campaign that has been carried out at LGCGM, the mechanical properties of Na-geopolymer are investigated as well as its cracking sensitivity at early age. This last depends on several parameters studied in the present project: tensile strength, Young's modulus, and delayed deformations such as autogenous shrinkage and basic creep. All of these parameters are characterized experimentally under autogenous condition. These results obtained for a Na-Geopolymer are compared to those of a Portland cement-based mortar. From restrained ring tests, it appears that the cracking sensitivity is lower for Na-Geopolymer. This behavior is mainly due to a low Young's modulus, a fast stabilization of autogenous shrinkage and a high creep capacity.

Keywords Autogenous shrinkage · Basic creep · Cracking · Mechanical performances · Na-geopolymer

1 Introduction

Geopolymer named by Joseph Davidovits in the late 1970s [1] is an inorganic material made by mixing aluminosilicates sources with an alkaline solution. Geopolymers structure consists of tetrahedral frameworks of AlO_4^- and SiO_4^- by linking together with oxygen bridges and with alkali metal ions balancing the charge associated with

H. Sounean (✉) · H. Kinda · D. Aveline
Laboratoire de Génie Civil et Génie Mécanique (LGCGM), Institut National des Sciences Appliquées de Rennes, Rennes, France
e-mail: sounean.heng@insa-rennes.fr

H. Kinda
e-mail: kinda.hannawi@insa-rennes.fr

D. Aveline
e-mail: aveline.darquennes@insa-rennes.fr

© RILEM 2021

F. Kanavaris et al. (eds.), *International RILEM Conference on Early-Age and Long-Term Cracking in RC Structures*, RILEM Bookseries 31, https://doi.org/10.1007/978-3-030-72921-9_14

165

tetrahedral Al [2, 3]. The general empirical formula of geopolymer is $Mn\{-(SiO_2)_z-AlO_2\}_n, wH_2O$ [2], where M is alkali metal cation (normally is Na^+ or K^+), and n is a degree of polycondensation with $z = 1, 2, 3$. Since several years, more and more research works focus on the design and the behavior of this inorganic material. Indeed, it presents several advantages: a low CO_2 release during its production [4–6], a high compressive strength, and a good chemical and fire resistance [7, 8].

The present study focuses on a Na-geopolymer designed to immobilize nuclear wastes such as Mg-Zr alloys fuel cladding used in the UNGG reactors (Uranium Natural Graphite Gas) in the framework of the DECIMAL project (Phenomenological Description Corrosion And Its Impact On The Durability Of Encapsulated Magnesium Wastes In Hydraulic Binders). In an aqueous media, Mg can corrode rapidly and lead simultaneously to hydrogen (H_2) release. But Rooses et al. [9] have shown that the corrosion of Mg-Zr immobilized in a Na-geopolymer matrix is low in comparison to an immobilization into a Portland cement matrix and further studies are being performed in the DECIMAL project to better describe the corrosion mechanisms of Mg alloys in this Na-matrix [10]. However, the chemical reactions driving geopolymerization are very complex and depend on many factors such as aluminosilicate source, curing time and temperature [11–13], nature and concentration of alkaline activator solution [14–16], as well as Si/Al/cation ratios [17, 18]. These parameters also affect the mechanical behavior of geopolymers at the macroscale. In the present study, the behavior of a Na-geopolymer is analyzed in autogenous condition to assess its cracking risk when its delayed deformations are restrained by an external element.

2 Materials and Curing Condition

To design the Na-geopolymer, a metakaolin is used as an aluminosilicates source. Its chemical composition is given in Table 1. Its area surface and specific density are equal to $17 \text{ m}^2/\text{g}$ and $2.4 \text{ g}/\text{cm}^3$ respectively.

The metakaolin-based geopolymer mortar -named MGEO hereafter- presents the following formulation: $1Na_2O-3.96SiO_2-1Al_2O_3-12.5H_2O$. The alkaline activator solution is prepared by mixing sodium silicate solution ($SiO_2 = 27.5 \text{ wt.}\%$, $Na_2O = 8.3 \text{ wt.}\%$, $H_2O = 64.2 \text{ wt.}\%$, $SiO_2/Na_2O = 3.42$) with sodium hydroxide pellets (>98 wt.% purity) and distilled water (conductivity = $25.43 \mu\text{s}/\text{cm}$ at $20 \text{ }^\circ\text{C}$, $\text{pH} = 7.66$). Moreover, sodium fluoride (1.25 M) used as corrosion inhibitor is also added, as well as quartz sand (0.315/1.6 mm). Furthermore, ordinary Portland cement mortar (CEM I 52.2 N) is used as a reference material and named hereafter MCEMI. It is mixed

Table 1 Chemical composition of metakaolin

Chemical	SiO_2	Al_2O_3	$K_2O + Na_2O$	Fe_2O_3	TiO_3	$CaO + MgO$
Metakaolin	55%	40%	0.8%	1.4%	1.5%	0.3%

with tap water (conductivity = 558.9 $\mu\text{s}/\text{cm}$ at 20 °C, pH = 8.06) and normalized sand (0/2 mm). The two studied mortars show the same paste volume and liquid to binder ratio ($L/B = 0.508$).

All the specimens are demolded after 24 h and stored at 20 ± 1 °C. The autogenous condition is obtained thanks to a double layer of aluminum foil. For mechanical tests, a plastic foil is also added between the adhesive aluminum foils and specimen. To control the autogenous condition, specimens' mass is regularly measured during all the tests.

3 Experimental Method

3.1 Mechanical Properties

To determine the tensile strength, a three-point flexural test is performed on three prismatic specimens ($4 \times 4 \times 16$ cm) with a loading rate of 0.01 mm/s. The tests are performed on 1, 3, 7, 28, and 90 days old specimens. After this test, specimens are loaded again to determine the compressive strength with a loading rate equal to 2.4 kN/s according to EN 196-1.

Young modulus test is carried out on three cylindrical specimens ($\phi 11 \times 22$ cm) at 3, 7, 28, and 90 days. Specimens are loaded with a rate of 0.5 MPa/s (NF EN 12390-4) until a value equal to 30% of their compressive strength determined previously on specimens having the same dimensions.

3.2 Autogenous Shrinkage

The autogenous shrinkage is measured on three prismatic specimens ($4 \times 4 \times 16$ cm) at their central axis by means of two inserts placed on each sample's extremities (top and bottom) with a displacement comparator from 1 to 40 days, as well as their mass loss.

In parallel, internal relative humidity evolution and water porosity are also measured to understand the autogenous shrinkage (amplitude and kinetics) as capillary depression is one of the main driving mechanisms responsible of this deformation. The internal relative humidity is monitored with a thermo-hygrometer sensor—having a precision of $\pm 2\%$ —placed weekly into the middle of cylindrical specimens ($\phi 50 \times 70$ mm) thanks to a drilled hole ($\phi 5 \times 35$ mm). To determine water porosity, three cylindrical 28 days old specimens ($\phi 40 \times 60$ mm) are water-saturated under vacuum for 44 h. Their mass is measured in air (M_{air}) as well as in water (M_{w}) thanks to the hydrostatic weighing. After, specimens are dried in an oven at 40 °C until to reach a constant mass value (M_{dry})—a mass variation inferior to 0.05% between to two measurements (24 h) is acceptable. Based on these measurements, bulk density

(ρ_{app}) and water porosity (ϕ) are calculated using the Eqs. (1) and (2) respectively:

$$\rho_{app} = \frac{M_{dry}}{M_{air} - M_w} \rho_w \quad (1)$$

$$\phi = \frac{M_{air} - M_{dry}}{M_{air} - M_w} \rho_w \quad (2)$$

With ρ_w the water density (1 g/cm^3).

3.3 Basic Creep

Compressive basic creep test is carried out on two prismatic specimens ($7 \times 7 \times 28$ cm) using hydraulic jacks. The total deformation is measured on each specimen side via two glued balls with a distance of 20 cm. A load equal to 20% of compressive strength previously determined on cylindrical specimens ($\phi 11 \times 22$ cm) is applied on 90 days old specimens. In parallel, autogenous shrinkage is also determined on unloaded samples ($7 \times 7 \times 28$ cm).

3.4 Restrained Ring Test

A ring test (Fig. 1) is performed to evaluate the cracking time of the studied mortars. Its steel ring is characterized by an inner (R_2) and outer (R_1) radius equal to 100 mm and 125 mm respectively. The outer radius (R_0) of the mortar ring cast around the steel ring is equal to 160 mm. The specimens are demolded after 24 h, and sealed

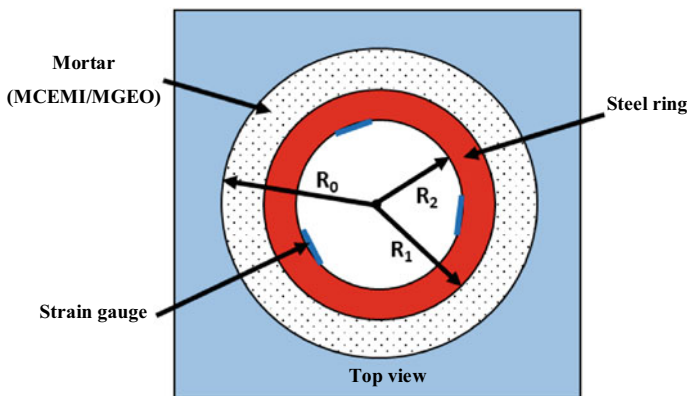


Fig. 1 Ring test setup

with a double layer of aluminum foils to obtain autogenous condition. The deformations of the steel ring are monitored thanks to three strain gauges glued at the mid-height of the inner surface of the steel ring (Fig. 1) and connected to the acquisition system. Moreover, the ambient temperature is also monitored to quantify the thermal deformation.

4 Experimental Results

4.1 Mechanical Properties

Figure 2 presents the flexural and compressive strength evolution for MCEMI and MGEO. According to Fig. 2a, the flexural strength of MGEO is lower than that of MCEMI for all the tested ages. It indicated that MGEO has lower tensile strength. It is probably related to the fact the geopolymer-based materials present an intrinsic brittleness due to their highly cross-linked framework [19]. The compressive strength of MGEO increases rapidly during the three first days (Fig. 2b). After 3 days, it evolves slowly and its value is close to the compressive strength of MCEMI. A similar evolution was found by Rocha et al. [20]. Figure 3 shows that the Young's modulus is lower for MGEO than for MCEMI at all the tested ages. This last behavior presents an advantage to limit the cracking risk of the geopolymer when its delayed deformations are restrained.

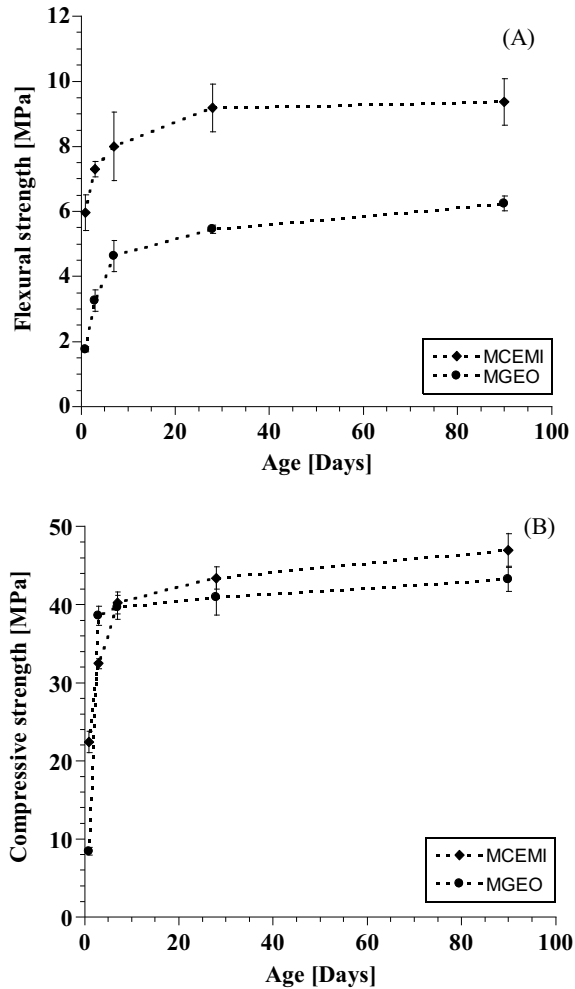
4.2 Autogenous Shrinkage

Figure 4 presents the autogenous shrinkage evolution of MGEO and MCEMI measured from 1 day. During the first 10 days, the autogenous shrinkage of MGEO evolves more rapidly. After, it slightly increases until 22 days. Beyond it tends to a constant value close to that obtained for MCEMI. For example, this deformation is equal to about 255 $\mu\text{m}/\text{m}$ for both mixtures at 22 days. Notice that the mass loss (because the tightness is not perfect after several weeks—unwanted drying) is slightly higher for MGEO at this age: 0.018% for MGEO and 0.007% for MCEMI. Moreover, the final deformation amplitude for MCEMI is quite similar than that found by Olivier [21] (230 $\mu\text{m}/\text{m}$ at 28 days for a mortar with W/C ratio equal to 0.5).

Water porosity

As one of the main mechanisms driving autogenous shrinkage for cementitious materials is the capillary depression, the water porosity was measured for the both studied mortars and the results at 28 days are presented in Table 2. It appears that MGEO is characterized by a more important porosity. In a next step, the pore size distribution

Fig. 2 Flexural (a) and compressive (b) strength for MCEMI and MGEO at 1, 3, 7, 28, and 90 days



will be characterized to better understand the effect of porosity on the autogenous deformation.

Internal relative humidity

On Fig. 4, the internal relative humidity evolution is also presented for both studied mortars. This parameter varies around a constant value ($\pm 95\%$) during the 40th days for MGEO, while it decreases progressively for MCEMI (89.6% at 43 days). Ma et al. [22] found a similar result for a fly-ash based geopolymer. They explain that by the decreasing of salt content (Na^+ and silicate species) in pore solution. Moreover, they assume that autogenous shrinkage of fly-ash based geopolymer is due to the continuous reorganization and polymerization of the gel structure instead of the self-desiccation process available for a classic cementitious material.

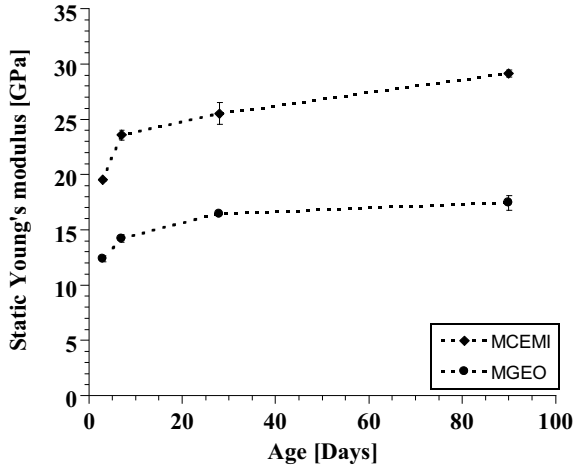


Fig. 3 Young’s modulus for MCEMI and MGEO at 3, 7, 28, and 90 days

Fig. 4 Evolution of internal relativity humidity (RH) and autogenous shrinkage (S) for MCEMI and MGEO

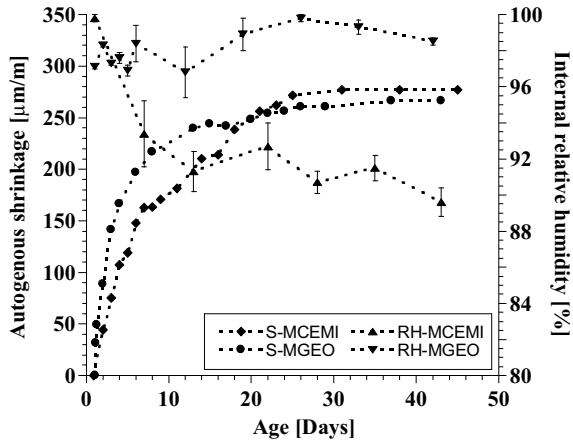


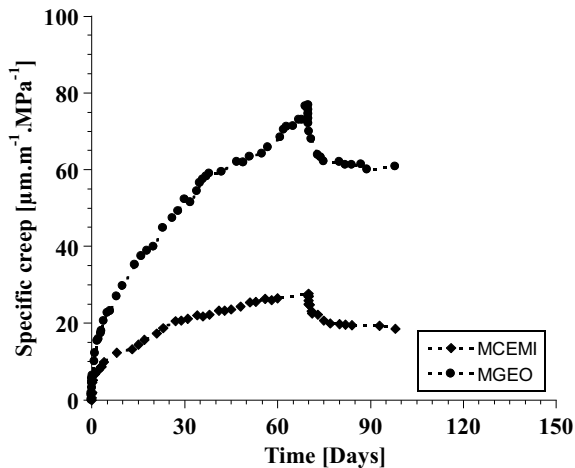
Table 2 Bulk density (ρ_{app}) and water porosity (ϕ) for MCEMI and MGEO at 28 days

Test	MCEMI	MGEO
ρ_{app} (g/cm ³)	1.989 ± 0.003	1.813 ± 0.002
ϕ (%)	20.9 ± 0.2	26.2 ± 0.5

4.3 Basic Creep

The specific basic creep is illustrated in Fig. 5 for both studied mortars loaded at 90 days. It is higher for MGEO. Thus, this mortar is characterized by a higher capacity to relax internal stresses—a positive behavior to reduce the cracking risk when the

Fig. 5 Specific basic creep of MCEMI and MGEO, loading at age 90 days



delayed deformations are restrained. The specimens were unloaded at 70 days. The residual deformation is also more important for MGEO. Notice that the mass loss at the test end is equal to 0.23% and 0.074% for MGEO and MCEMI respectively.

4.4 Restrained Ring Test

To determine the cracking sensitivity, a restrained ring test was performed. The deformation evolutions of the steel ring surrounded by MCEMI and MGEO during the first 30 days are showed in Fig. 6. During these tests, the average ambient temperature is equal to 18.6 ± 1 °C and 19.7 ± 1 °C respectively. The deformation increases more rapidly for MGEO at early age, but their amplitude from 5 days is quite similar. At about 25 days, MCEMI cracks whereas no crack is observed for MGEO beyond 30 days. Based on these results, it appears that MGEO presents a lower cracking sensitivity when its delayed deformations are restrained.

5 Conclusion

The main objective of this experimental campaign is to study the delayed behavior of a Na-geopolymer and its cracking risk under autogenous condition. This material presents a low Young's Modulus and a low tensile strength. Even though the lower stiffness can reduce the internal stresses amplitude, a lower tensile strength may cause a higher cracking risk. However, the delayed deformation results show that Na-geopolymer is characterized by a rapid stabilization of autogenous shrinkage reaching a constant after 22 days and a high specific basic creep. These both results

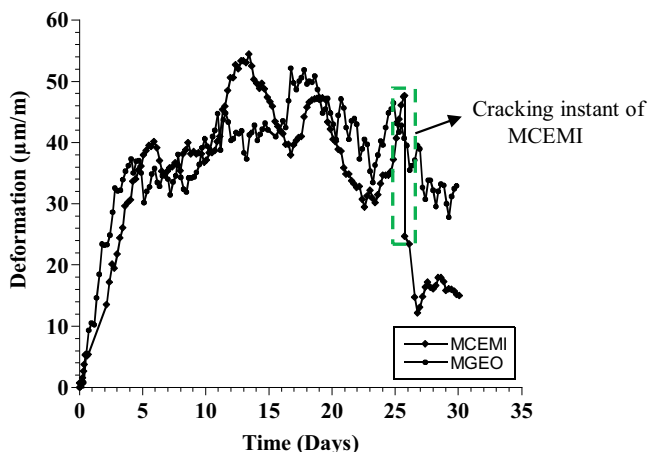


Fig. 6 Steel ring deformations due to the delayed deformations of MGEO and MCEMI under autogenous condition

are interesting to limit cracking sensitivity when the delayed deformations of the geopolymer are restrained. Thanks to a ring test coupling all these material parameters, the cracking sensitivity of the geopolymer was studied. This test has confirmed that the studied geopolymer presents a lower cracking sensitivity in comparison to a classic Portland cement mortar.

Acknowledgements Work performed within the Investments for the future program of the French Government and operated by French National Radioactive Waste Management Agency (Andra).

References

1. Davidovits, J.: The need to create a new technical language for the transfer of basic scientific information. Conference 1982, Transfer and Exploitation of Scientific and Technical Information, vol. 1, pp.19–23. Luxemburg (1982)
2. Davidovits, J.: Geopolymer: inorganic polymeric new materials. *J. Therm. Anal.* **37**, 1633–1656 (1991)
3. Duxson, P., Luckey, G.C., Separovic, F., Van Davenport, J.S.J.: Effect of alkali cations on aluminum incorporation in geopolymer gels. *Ind. Eng. Chem. Res.* **44**, 832–839 (2005)
4. Duxson, P., Provis, J.L., Luckey, G.C., Van Davenport, J.S.J.: The role of inorganic polymer technology in the development of green concrete. *Cem. Concr. Res.* **37**, 1590–1597 (2007)
5. Provis, J.L., Van Davenport, J.S.J.: *Geopolymers: Structures, Processing Properties and Industrial Applications*. Boca Raton, Boston, New York, Washington (2009)
6. McLellan, B.C., William, R.P., Lay, J., van Riessen, A., Corder, G.D.: Costs and carbon emission for Geopolymer pastes in comparison to ordinary Portland cement. *J. Clean. Prod.* **19**(9–10), 1080–1090 (2011)

7. Barkarev, T.: Resistance of geopolymer materials to acid attack. *Cem. Concr. Res.* **35**, 658–670 (2005)
8. Fernández-Jiménez, A., Palomo, A.: New cementitious materials based on alkali-activated fly ash: performance at high temperatures. *J. Am. Ceram. Soc.* **91**(10), 3308–3314 (2008)
9. Rooses, A., Lambertin, D., Chartier, D., Frizon, F.: Galvanic corrosion of Mg-Zr fuel cladding and steel immobilized in Portland cement and geopolymer at early ages. *J. Nucl. Mater.* **435**, 137–140 (2013)
10. Boubon, R., Deschanel, X., Cabié, M., Rébiscoul, D.: Evolution of corrosion products formed during the corrosion of MgZr alloy in poral solutions extracted from Na-geopolymers used as conditioning matrix for nuclear waste. *Materials* **13**, 4958 (2020)
11. Van Jaarsveld, J.G.S., Van Daventer, J.S.J., Luckey, G.C.: The effect of composition and temperature on the properties of fly as- and kaolinite-based geopolymers. *Chem. Eng. J.* **89**, 63–73 (2002)
12. Rovananik, P.: Effect of curing temperature on the development of hard structure of metakaolin-based geopolymer. *Constr. Build. Mater.* **24**, 1176–1183 (2010)
13. Basil, S.A., Tareq, S.A.: Effect of curing system on metakaolin based geopolymer concrete. *J. Babylon Univ./Eng. Sci.* **3**(24) (2016)
14. Provis, J.L., Duxson, P., Luckey, G.C., Separovic, F., Kriven, W.M., Van Daventer, J.S.J.: Modeling speciation in highly concentrated alkaline silicate solutions. *Ind. Eng. Chem. Res.* **44**, 8899–8908 (2005)
15. White, C.E., Provis, J.L., Llobet, A., Proffen, T., Van Daventer, J.S.J.: Evolution of local structure in geopolymer gels: An in situ neutron pair distribution function analysis. *J. Am. Ceram. Soc.* **94**(10), 3532–3539 (2011)
16. Fan, Z., Liying, Z., Ming, L., Chenzhong, M., Yen, N.L., Xiao, H.: Role of alkali cation in compressive strength of metakaolin based geopolymer. *Ceram. Int.* **43**, 3811–3817 (2017)
17. Bourlon, A.: Phys Physico-chimie et rhéologie de géopolymères frais pour la cimentation des puits pétroliers. Thèse de doctorat: Physique et Chimie des Matériaux, Paris: Université Pierre et Marie Curie (2011)
18. Duxson, P., Fernández-Jiménez, A., Provis, J.L., Luckey, G.C., Palomo, G.C., Van Daventer, J.S.J.: Geopolymer technology: the current of the art. *J. Mater. Sci.* **42**, 2917–2933
19. Pan, Z., Sanjayan, J.G., Rangan, B.V.: Fracture properties of geopolymer paste and concrete. *Mag. Concr. Res.* **63**(10), 763–771 (2011)
20. Rocha, T.S., Dias, D.P., França, F.C.F., Guerra, R.R.S., Marques, L.R.C.O.: Metakaolin-based geopolymer mortars with different alkaline activators (Na⁺ and K⁺). *Constr. Build. Mater.* **178**, 453–461 (2018)
21. Olivier, K.: Etude expérimentale et modélisation de l’auto-cicatrisation des matériaux cimentaires avec additions minérales. Thèse de doctorat: Sciences mécanique et énergétiques, matériaux et géosciences, l’Université de Sherbrooke et de l’Université Paris-Saclay (2016)
22. Ma, Y., Ye, G.: The shrinkage of alkali activated fly ash. *Cem. Concr. Res.* **68**, 75–82 (2015)